Neurobiology of Pain 6 (2019) 100030

Contents lists available at ScienceDirect

Neurobiology of Pain

journal homepage: www.elsevier.com/locate/ynpai

Original Research

Chronic pain after blast-induced traumatic brain injury in awake rats

Olivia Uddin[a,1], Paige E. Studlack[a,1], Saitu Parihar[a,1], Kaspar Keledjian[b], Alexis Cruz[a], Tayyiaba Farooq[a], Naomi Shin[a], Volodymyr Gerzanich[b], J. Marc Simard[b,c,d], Asaf Keller[a,*]

[a] Department of Anatomy and Neurobiology and Program in Neuroscience, University of Maryland School of Medicine, 20 Penn St, HSF-II S251, Baltimore, MD, USA
[b] Department of Neurosurgery, University of Maryland School of Medicine, 10 S Pine St, MSTF 634B, Baltimore, MD, USA
[c] Department of Pathology, University of Maryland School of Medicine, 10 S Pine St, MSTF, Room 634B, Baltimore, MD, USA
[d] Department of Physiology, University of Maryland School of Medicine, 10 S Pine St, MSTF, Room 634B, Baltimore, MD, USA

ARTICLE INFO

Keywords:
Blast-TBI
Chronic pain
Rat grimace scale
Posterior thalamus
Spinal trigeminal nucleus caudalis

ABSTRACT

Explosive blast-induced traumatic brain injury (blast-TBI) in military personnel is a leading cause of injury and persistent neurological abnormalities, including chronic pain. We previously demonstrated that chronic pain after spinal cord injury results from central sensitization in the posterior thalamus (PO). The presence of persistent headaches and back pain in veterans with blast-TBI suggests a similar involvement of thalamic sensitization. Here, we tested the hypothesis that pain after blast-TBI is associated with abnormal increases in activity of neurons in PO thalamus. We developed a novel model with two unique features: (1) blast-TBI was performed in awake, un-anesthetized rats, to simulate the human experience and to eliminate confounds of anesthesia and surgery inherent in other models; (2) only the cranium, rather than the entire body, was exposed to a collimated blast wave, with the blast wave striking the posterior cranium in the region of the occipital crest and foramen magnum. Three weeks after blast-TBI, rats developed persistent, ongoing spontaneous pain. Contrary to our hypothesis, we found no significant differences in the activity of PO neurons, or of neurons in the spinal trigeminal nucleus. There were also no significant changes in gliosis in either of these structures. This novel model will allow future studies on the pathophysiology of chronic pain after blast-TBI.

1. Introduction

Blast-induced traumatic brain injury (blast-TBI) is a prevalent and serious trauma affecting U.S military personnel. Explosive blasts are responsible for 72% of service member TBI cases (Dobscha et al., 2009), and blast-TBI patients incur medical costs four times greater than other veterans treated at Veterans Affairs hospitals (Taylor et al., 2012). Adding to this higher treatment burden, TBI often precedes chronic neurological and psychological disorders. Nearly 74% of veterans with mild blast-TBI suffer chronic pain, with headaches and back pains being the most common complaints (Belanger et al., 2009; Patil et al., 2011; Strigo et al., 2014). These patients frequently suffer also from post-traumatic stress disorder (PTSD), a co-morbidity that is particularly impactful on quality-of-life and that increases healthcare burden (Taylor et al., 2012; Polusny et al., 2011; Dobscha et al., 2009; Lew et al., 2009; Ruff et al., 2008).

Despite the large number of veterans suffering from anxiety and chronic pain after blast-TBI (TBI-Pain), few studies have sought to elucidate the underlying pathophysiology. In clinical studies of mild blast-TBI survivors, resting-state functional magnetic resonance imaging revealed increased activity of brain regions associated with pain, particularly enhancement of thalamocortical connectivity (Tang et al., 2011; Venkatesan et al., 2015; Zhu et al., 2014). These findings suggest the involvement of CNS sensitization in TBI-Pain.

We previously demonstrated that thalamic sensitization is causally involved in chronic pain after SCI (Keller and Masri, 2014; Masri et al., 2009; Masri and Keller, 2012). Migraine studies report similar increases in activity of the thalamic neurons in both patient populations and animal models (Burstein et al., 2010; Noseda and Burstein, 2013). Because blast-TBI patients report similar headache features as chronic migraineurs, we hypothesized that abnormal increases in spontaneous and evoked activity of thalamic neurons are associated with TBI-Pain.

TBI-pain may also result from abnormalities in the periaqueductal gray (PAG) and rostral ventral medulla (RVM), key structures in the descending pain modulatory pathways (Bannister and Dickenson, 2017; Ossipov et al., 2014; Mason, 2011; Heinricher et al., 2009). The PAG is particularly vulnerable to primary blast injury, due to its proximity to the aqueduct (Cernak and Noble-Haeusslein, 2010; Jang et al., 2016);

* Corresponding author at: Department of Anatomy and Neurobiology, 20 Penn St, HSF-II S251, Baltimore, MD 21201, USA.
E-mail address: akeller@som.umaryland.edu (A. Keller).
[1] OU,PES,SP contributed equally to the manuscript.

https://doi.org/10.1016/j.ynpai.2019.100030
Received 16 November 2018; Received in revised form 14 February 2019; Accepted 1 April 2019
Available online 02 April 2019
2452-073X/ © 2019 The Authors. Published by Elsevier Inc. This is an open access article under the CC BY-NC-ND license (http://creativecommons.org/licenses/BY-NC-ND/4.0/).

Blast waves cause exaggerated damage due to spallation at tissue borders of different densities, such as this periventricular area (Elder et al., 2010; Nakagawa et al., 2011; Cernak and Noble-Haeusslein, 2010; Rosenfeld et al., 2013; Shively et al., 2016). Because the PAG is involved in both cognitive and emotional control of pain, we predicted that persistent pain and anxiety behavior would be associated with persistent glia-mediated inflammation in PAG and its downstream target, the RVM.

Current models of blast-TBI are not ideal for studying the mechanisms of pain due to the use of anesthetics and surgical procedures (Warner et al., 1991; Kapinya et al., 2002; Lee et al., 2008; Park et al., 2009; Hara and Harris, 2002). Therefore, we modified our previously described model of direct cranial blast injury (dcBI) (Kuehn et al., 2011; Studlack et al., 2018) to expose awake, un-anesthetized rats to an explosive blast. By exposing rats to the dcBI model without anesthesia, we test the hypothesis that blast-TBI will induce glia-mediated inflammation to sensitize the thalamus, resulting in elevated pain and hyperalgesia.

2. Methods

All procedures were conducted according to Animal Welfare Act regulations and Public Health Service guidelines. Strict aseptic surgical procedures were used, according to the guidelines of the International Association for the Study of Pain, and approved by the University of Maryland School of Medicine Animal Care and Use Committee. A total of 38 adult male Long-Evans rats (250–300 g; Harlan, Indianapolis, IN) and 37 adult male Wistar rats (250–325 g; Harlan, Indianapolis, IN) were used in this study. Unlike Long Evans rats, Wistar rats have white hair and red eyes, which creates a contrast that facilitates facial grimace analysis.

Animals were randomly allocated to experimental or control groups. In all experiments, the investigators were blinded to animal condition. A coded key of all specimens evaluated was kept and not shared with the investigators performing the experiments until data analysis was completed. Thus, allocation, concealment, blinded conduct of the experiment, and blinded assessment of the outcomes was performed.

2.1. Cranium only blast injury in awake rats

Rats were trained to place their head through the Blast Dissipation Chamber Cranium Interface, BDCCI, which is described in our previous studies (Kuehn et al., 2011; Studlack et al., 2018). Rats were placed in a behavior chamber (Fig. 1) with access to a positive reward (sweetened milk). The reward was delivered through a feeding tube situated on the opposite side of the BDCCI. At all times, the animals could voluntarily approach and freely withdraw from the feeding tube. Training was discontinued when rats place their head into the BDCCI chamber continuously for at least 30 s to access the reward. The apparatus was cleaned after each session with Roccal-D disinfectant and wiped dry. Rats were acclimated to the chamber for one to two weeks and, on each day, training was performed at the same time.

Prior to each training session, rats were food fasted for 12 h. A recovery day from the fasting was included between the training sessions to minimize nutritional differences from normal food routine. The animals were returned to regular diet after the fasting period. Diet was provided *ad libitum* on recovery day. Water was available *ad libitum* before and after testing sessions. During the food restriction phase, animals were weighed daily to ensure that their body weight did not fall below 85% of the baseline.

Animals received one blast-TBI following the completion of training. The blast required no surgical procedures. Rats were placed in the behavior chamber used in the training phase. When the rat placed its head against the end of the blast dissipation chamber (BDC) centered over the occipital crest for at least five seconds, a blast wave was applied, as previously described (Kuehn et al., 2011; Studlack et al., 2018). We have studied this model of posterior cranium blast exposure extensively (Hayman et al., 2018). We showed that high intensity blast exposure (> 800 kPa) at the foramen magnum in anesthetized rats is associated with a high incidence of subdural hematomas and high mortality, whereas the same exposure rostral to and not involving the foramen magnum is associated with minimal hemorrhage and minimal mortality (see Results). When the foramen magnum area is involved, the relationship between blast intensity and morbidity/mortality is a very steep sigmoidal, with half-maximum ~ 750 kPa (see Results). In the present paper, we used an exposure of 500 kPa in awake rats, produced using a level four charge and a BDC of 27 cm in length, which we reported results in minimal hemorrhage and no mortality. The impact produced by the blast wave at this intensity caused downward movement of the head, but did not produce skull damage, bleeding or skin lacerations.

Immediately following the blast, we noted the location of injury, assessed by noting the location of gunpowder residue. For the remainder of the study we included only rats that received blast-TBI in the posterior cranium – in the region of the occipital crest and behind the foramen magnum. We also recorded changes in the following physical abnormalities: number of seizure-like body contractions (contractions), forelimb and hindlimb weakness measured with grip strength assessments, and the steepest angle at which the rat can climb an inclined slope (inclined plane). Rats were observed closely for at least one hour for any other physical side effects. We continued to monitor them daily thereafter.

2.2. Behavioral confirmation of anxiety, pain, and hyperalgesia

All animals were tested for ongoing pain and hypersensitivity to thermal and mechanical stimuli at least three weeks after injury induction with blast exposure. To minimize the animals' anxiety, they were habituated before behavioral testing and trained with the use of rewards (i.e., milk and rat treats).

2.2.1. Measuring anxiety-like behavior with the elevated plus maze

Anxiety-like behavior was assessed in an elevated plus maze (Coulbourn Instruments, Holliston, MA) comprised of two intersecting arms measuring 10 by 50 cm, one of which was an open platform and the other closed with walls 30 cm high. The maze was 55 cm off the ground. Rats were placed in the center of the maze, facing an open arm, and filmed overhead for 5 min. Time spent in the open arms was quantified by Any Maze video tracking software (Stoelting, Wood Dale, IL). Rats were considered to be in an open arm if their head and body to at least the fore-limbs was on an open arm.

2.2.2. Spontaneous pain analysis with rat grimace scale

Rat grimace scores were determined based on methods described by Sotocinal et al. (2011) and in our previous study (Akintola et al., 2017). Rats were habituated to a Plexiglass chamber measuring $10 \times 20 \times 14$ cm and, on the next day, filmed in the chamber for 30 min. Using Rodent Face Finder software, 10 images from each video were randomly selected, coded, and scrambled to maintain experimenter blindness. We then scored the images for three action units: orbital tightness, nose and cheek flatness, and ear folding. Rat grimace scores were determined as the mean score of the three action units for each image, averaged by rat. We did not score changes in whisker position, due to low predictive validity and inter-rater reliability in pilot studies. Instead, we averaged the three action unit scores to obtain a rat grimace score for each rat to compare spontaneous pain following blast injury in sham and blast-TBI groups.

2.2.3. Facial thermal sensitivity

We quantified facial thermal sensitivity with the orofacial pain assessment device (OPAD, Stoelting), using methods previously described (Neubert et al., 2006). The OPAD establishes an operant conflict

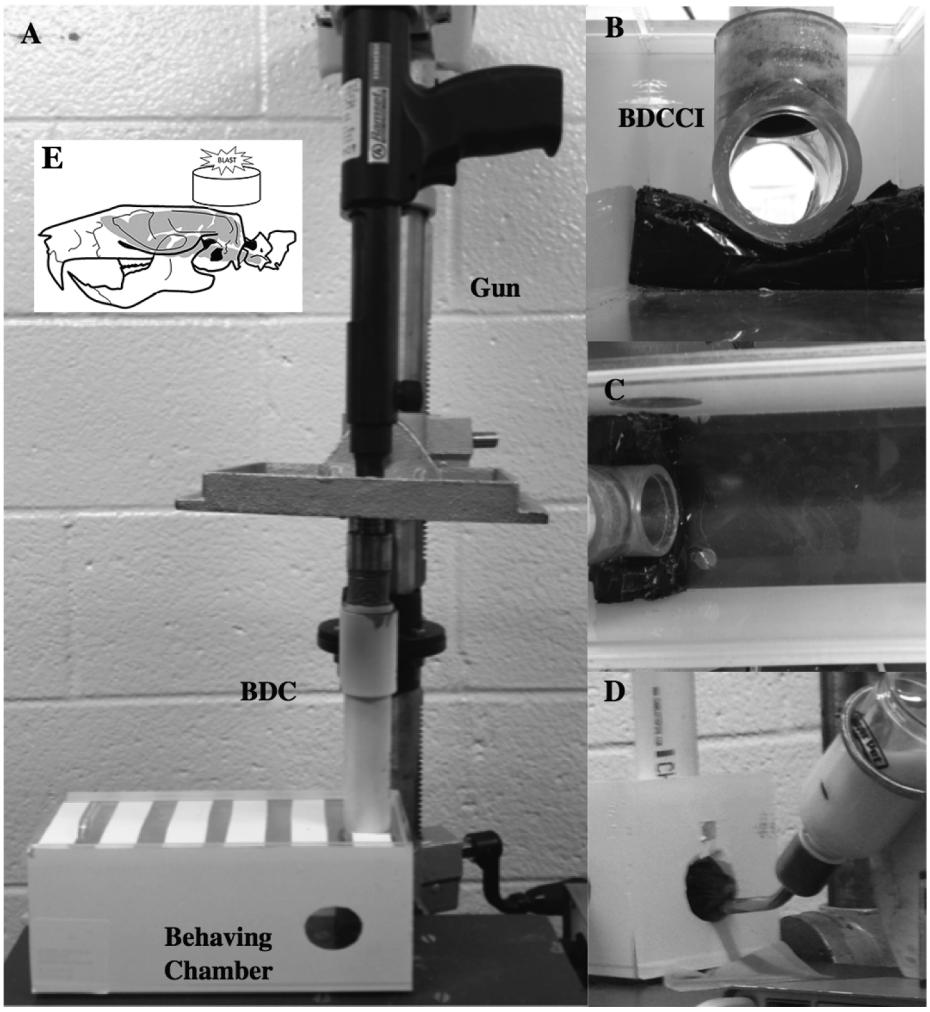

Fig. 1. Cranium Only Blast Injury Apparatus (COBIA) A: Photograph of the COBIA showing the vertically-oriented gun interfacing with the blast dissipation chamber (BDC) that connects to the BDC-cranium interface (BDCCI). B, C: Views of the BDCCI placed in the behaving chamber. D: Photograph of rat properly placing head through the BDCCI. E: Schematic depicting the location of the collimator over the foramen magnum.

paradigm that creates a behavioral outcome where an animal must decide between receiving a reward and escaping a noxious stimulus. Unlike reflexive withdrawal measures, this approach relies on operant behavioral strategies, involving cortical structures, to initiate a motivated behavior that terminates exposure to the noxious stimulus. This strategy overcomes many of the pitfalls associated with more traditional, reflexive behaviors, which often employ only spinal reflex loops to govern a withdrawal response from noxious stimuli without assessing higher order pain processes (Mogil, 2009). Rats were habituated and trained to drink sweetened milk in the OPAD chamber, which is a closed plexiglass chamber with a small gap surrounded by thermodes, which can be controlled to adjust the temperature. Rats were trained to place their heads through this gap and come in contact with the thermodes through the incentive of a reward on the other side. During the training phase, which lasted for approximately a week, the thermodes were set to 27 °C. Following training, rats had one testing session per day for 3 days. Each testing session lasted 10 min, during which the temperature of the thermodes was randomly set to 7, 37, 45, or 50 °C. The order in which the testing was performed at these temperatures was randomized for each rat. The animals voluntarily approached the feeding tube, and could freely withdraw from the thermodes and feeding tube at any time. An AnyMaze (Stoetling) module for OPAD analysis was used to quantify the number of times the rats made contact with the thermodes, the number of licks of the reward, and the amount of reward consumed. Fur on the buccal regions was shaved for these experiments.

2.2.4. Facial mechanical withdrawal thresholds

We acclimated rats to a process in which an experimenter wrapped their bodies with a small towel, leaving the head exposed, and holding the wrapped rat in their arms. After several habituation sessions, mechanical hyperalgesia of the facial skin was assessed by applying calibrated von Frey filaments to the center of the whisker-pad in the infraorbital branch of the trigeminal nerve receptive field, which is also the region of face in contact with the thermodes during OPAD trials. The level of mechanical sensitivity was quantified as the average withdrawal threshold (g), using the Up-Down method described by Dixon (1965). Positive responses to the filaments were characterized by an abrupt movement of the head away from the filament, vocalization, or an attempt to bite the filament. A lower withdrawal threshold denotes higher sensitivity.

2.2.5. Hind-paw mechanical withdrawal thresholds

Rats were tested for their mechanical sensitivity using calibrated von Frey filaments, ranging from 0.008 to 300 g of force, applied to the plantar surface of the hind-paws. Quick withdrawal or licking of the paw in response to the stimulus was considered a positive response. Filaments were continuously applied for at least 20 applications with a 1–2 min interval between stimuli, using the previously described Up-Down method (Dixon, 1965).

2.3. In vivo extracellular recordings

At least 4 weeks after the blast-TBI, non-recovery surgical procedures were used to prepare for extracellular recordings. Rats were initially anesthetized (60 mg/kg ketamine and 7.5 mg/kg xylazine given IP) to insert a jugular catheter, as in our previous studies (Whitt et al., 2013). We delivered an intravenous infusion of urethane (1.5 mg/kg) through the jugular catheter, to control the level of anesthetic, which was kept at level III-2 (Friedberg et al., 1999). We selected urethane because it has negligible effects on glutamatergic and GABAergic transmission, and therefore produces only minimal disruption of signal transmission (Sceniak and Maciver, 2006). Anesthetic levels were monitored by continually recording electrocorticograms (ECoGs) using a pair of screws implanted in the skull. For PO recordings, small craniotomies (1–2 mm^2) provided access for recording electrodes based on stereotaxic coordinates (at approximately AP 3.2 mm, ML 2.6 mm relative to bregma), as reported in our previous studies (Masri et al., 2009; Whitt et al., 2013). For recordings from spinal trigeminal nucleus caudalis (SpVc), a laminectomy was performed, including the axis and part of the occipital bone, as previously described (Okubo et al., 2013).

Recordings were made through a custom-made platinum tungsten fiber electrode (< 5 µm tip diameter, 2–4 MΩ resistance). Once a single unit was well isolated, spontaneous activity was recorded for at least 3 min, followed by evoked activity in response to either innocuous or noxious stimuli.

2.3.1. Vibrissae, face, and hind-paw stimulation

We recorded responses of single units to a series of stimuli applied with mechanical forces that spanned the innocuous and noxious range. We stimulated vibrissae with innocuous air puffs delivered with a Picospritzer, as in our previous studies (Masri et al., 2008). This method produces highly reproducible stimuli, allowing quantitative analyses of stimulus/response relationships. Other regions of the head, face, and hind- paw were stimulated using a calibrated electronic von Frey esthesiometer (IITC, Woodland Hills, CA). The esthesiometer was manually applied to the receptive area with increasing force over a 2 s period. Forces spanned the innocuous and noxious range (0–200 g, tip diameter 0.8 mm). Stimuli were applied at least 10 times to the receptive field of each recorded neuron. We computed evoked firing rate during each application of mechanical stimulation. Analog signals from the esthesiometer were digitized and the integral of the pressure waveform computed using algorithms custom written in Matlab (MathWorks, Natick, MA). To determine neuronal response magnitudes, we divided the difference in firing rate evoked in response to the stimulus over baseline firing rate by the integral of the stimulus waveform.

In addition to the noxious mechanical stimulation induced with the esthesiometer, we assessed neuronal responses to noxious thermal stimulation to the face. We placed the tip of a dental surgical laser (Picasso Lite, AMD Lasers, LLC, Indianapolis IN 46240) set to 2 Watts cycling on and off at 30 msec intervals for several seconds in close proximity to the skin of the whisker-pad and cheeks. This produced a temperature of 45 °C, determined by recording from intradermal probes.

2.3.2. Single unit analyses

Waveforms were digitized (40 kHz) through an OmniPlex data acquisition system (Plexon, Dallas, TX), and sorted as units offline with Offline Sorter (Plexon), using dual thresholds and principal component analyses. We generated autocorrelograms with Neuroexplorer software (Plexon) to confirm that we obtained recordings from single units. We exported time stamps of well-isolated units, stimulus triggers and waveforms to Matlab (MathWorks) for analyses using our library of custom-written algorithms. Significant responses were defined as bins in which activity is significantly greater (99% confidence interval) than the mean baseline-firing rate.

2.4. Histology

Following the electrophysiological recording session, animals were deeply anesthetized and transcardially perfused with buffered saline followed by 4% buffered paraformaldehyde. We obtained 60 µm-thick coronal brain sections and Nissl-stained them. Sections were collected based on craniotomy site coordinates and histological landmarks as previously described (Masri et al., 2009; Whitt et al., 2013). The obex was used as an additional landmark for SpVc section collection. The sections were examined with a transmission microscope to identify recording sites within the posterior nucleus of the thalamus (PO) or SpVc; marked with lesions. All recordings sites were reconstructed and only neurons with confirmed placement within the desired nucleus were included in analysis.

2.4.1. Immunohistochemistry

Rats were transcardially perfused with 4% paraformaldehyde, brains were removed, placed in fixative overnight, and cryoprotected with 30% sucrose for up to one week. After embedding in Tissue-Tek OCT compound (Sakura Finetek, Torrance, CA), 10 µm sagittal cryosections were mounted on slides, washed with 0.4 M phosphate-buffered saline (PBS), blocked in 2% donkey serum with 0.2% Triton X-100 (Sigma-Aldrich, St. Louis, MO) in PBS for 1 h. Sections were then incubated overnight with primary antibody directed against rabbit anti-ionized calcium-binding adapter molecule 1 (Iba1, 1:500, 019-19741, Wako Pure Chemical Industries, Richmond, VA) and mouse anti-glial fibrillary acid protein (GFAP, 1:500, C9205, Sigma-Aldrich). For secondary fluorescent labeling, the sections were washed 3 times in PBS, then incubated in the dark. After 1 h, the slides were washed, dried and covered with Prolong Antifade reagent with 4,6-diamino-2-phenlindole (DAPI, P-36931, Life Technologies, Grand Island, NY). Low- and high-power photomicrographs were taken using a Nikon Eclipse 90i camera, and images were adjusted for brightness and contrast using NIS software (Nikon Instruments Inc., Melville, NY).

For quantitative immunohistochemistry of PO and SpVc regions-of-interest (ROI), all sections were immunolabeled as a single batch. All images were collected using uniform parameters of magnification and exposure. Analysis was performed using NIS software (Nikon) by computing % ROI or cell counts within a specified ROI for each of the markers (GFAP or Iba1). For GFAP in PO and SpVc, specific labeling was defined as pixels with signal intensity greater than twice that of background, and the area occupied by pixels with specific labeling was used to determine the percent area with specific labeling (% ROI). For Iba1 in PO and SpVc, the nuclei with specific labeling in the ROI were counted.

Glia labeling in the PAG and RVM was determined in a separate cohort of blast-exposed rats. Brains for this experiment were collected from paraformaldehyde-perfused rats, 15–16 weeks after injury. After overnight fixation, brains were stored in PBS until sectioning. Coronal sections, 50 µm, through the PAG and RVM were collected and free-floating sections were labeled with the following: double-labeling with mouse anti-GFAP conjugated to a CY3 fluorophore (1:10,000, C9205, Sigma) and rabbit anti-Iba1 (1:10,000, 019-19741, Wako Pure Chemical Industries, Richmond, VA) and goat anti-rabbit secondary antibody with 488 nm fluorophore (1:1500; 4412, Cell Signaling Technology, Danvers, MA).

2.5. Statistical analysis

Unless otherwise noted, values given are median ± 95% confidence interval. We performed statistical analysis in GraphPad Prism version 7.00 for Mac (GraphPad Software, La Jolla). Since the data were not normally distributed, we assessed statistical significance using a Mann-Whitney U ranked-sum test. We used a Kruskal-Wallis test to evaluate post-TBI contractions. A p value < 0.05 was considered to be statistically significant. For all analyses, we used individual animals as

samples, averaging all measurements obtained from an animal. For example, we averaged firing rates of all neurons recorded from a single animal and present that average as a single sample.

3. Results

3.1. Acute effects of TBI-pain

We used several criteria to classify the severity of TBI immediately after the blast. We included only rats that received blast-TBI in the posterior cranium, in the region of the occipital crest and over the foramen magnum. Using the Cranium Only Blast Induced Apparatus (COBIA) model with anesthetized rats, we have shown that neurofunctional outcomes and severity of subdural hemorrhage due to blast injury are worse when blasts are directed over this region, as compared to more rostral points (Hayman et al., 2018).

Blast-TBI resulted in muscle weakness and short-lived motor impairment in the recovery period following the blast injury (lasting about an hour), that was corroborated with grip strength measures. Forelimb grip strength was significantly impaired in blast-TBI rats (n = 23, median = 826 g, 95% CI = 743–883) over sham rats (n = 21, median = 1050, 95% CI = 868–1106; Mann-Whitney U = 125.5; p = 0.006, Fig. 2). Hindlimb grip strength was even more severely impaired: blast-TBI rats (n = 24) had median grip strength of 311 g (95% CI = 233–359), while sham-injured rats (n = 21) were 60% stronger (median = 497, 95% CI = 420–565, Mann-Whitney U = 48, p < 0.0001, Fig. 2). Blast-exposed rats also had reduced ability to climb a steep inclined plane, compared to sham rats (blast-TBI: n = 45, median = 60, 95% CI = 58–65; sham: n = 28, median = 70, 95% CI = 60–73; Mann-Whitney U = 365; p = 0.002; Fig. 2).

Injured rats had contractions that lasted less than 60 s after the blast, with no strain effect between Long Evans (LE, n = 23) and Wistar rats (Wis, n = 27) (LE median = 15, 95% CI = 5–30; Wis median = 20, 95% CI = 15–28; Kruskal-Wallis test with Dunn's multiple comparisons; p = 0.93, Fig. 2).

3.2. Persistent anxiety

To test for persistent anxiety-like behaviors, rats at 4–5 weeks after injury were placed in an elevated plus maze and allowed to freely explore closed, walled arms or open arms. Rats in the blast-TBI group (n = 8) spent a median 5.4% (95% CI = 1.6–15.9) of the time in the open arms, largely preferring the closed arms. Sham-injured rats (n = 10) spent significantly more of the trial time exploring the open arms (median = 13.6%, 95% CI = 7.5–28.5), compared to blast-TBI animals (Mann-Whitney U = 15; p = 0.03; Fig. 3).

3.3. Ongoing pain

Blast-TBI in humans is associated with increased sensitivity to painful stimuli and chronic pain, particularly in the head and back (Rosenfeld et al., 2013; Sayer, 2012; Tham et al., 2013). To determine if similar outcomes occur in our animal model, we compared blast-TBI and sham rats using tests of ongoing pain and hyperalgesia.

We quantified facial grimace, an established metric of ongoing pain in both humans and animal models of pain (Langford et al., 2010; Sotocinal et al., 2011; Matsumiya et al., 2012; De Rantere et al., 2016; Akintola et al., 2017). In a previous study using an orofacial neuropathic pain model (chronic constriction injury of the infraorbital nerve, CCI-ION), we showed that Rat Grimace Scale (RGS) scores were increased 10 and 27 days after injury (Akintola et al., 2017). In the present study, sham RGS scores were similar to baseline RGS scores of naive rats, reported in our prior study, and we also found that 4–5 weeks after blast-TBI, increases in RGS scores were comparable to the increases seen after CCI-ION. As an average of scores for the orbital tightening, nose and cheek flattening, and ear position change action units (see Methods), we compared RGS scores for blast-injured and sham rats 4–5 weeks after injury. RGS scores were significantly elevated in blast-TBI (n = 13, median = 0.83, 95% CI = 0.61–1.15) compared to sham rats (n = 25, median = 0.6, 95% CI = 0.35–0.73; Mann-Whitney U = 86, p = 0.02; Fig. 3). The significantly higher RGS scores in blast-TBI rats suggest that they endure ongoing pain for at least 4 weeks after blast injury.

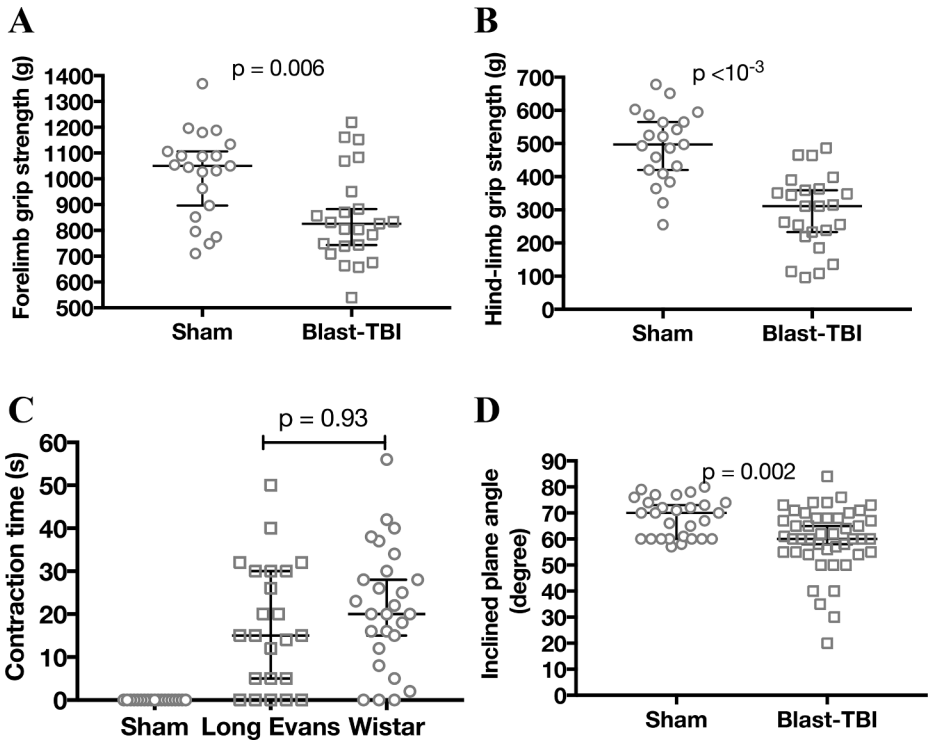

Fig. 2. Early motor deficits after blast-TBI. A, B: Grip strength measurements 10 min after blast injury demonstrate an early motor deficit in both the fore-limbs and hind-limbs. C: Immediately following blast-TBI, rats of both the Long Evans and Wistar strains have seizure-like body contractions. D: Maximum inclined plane angle climbed after blast-TBI is significantly lower in rats exposed to blast compared to sham-injured rats. Here and elsewhere, individual data are depicted, along with medians and 95% confidence intervals.

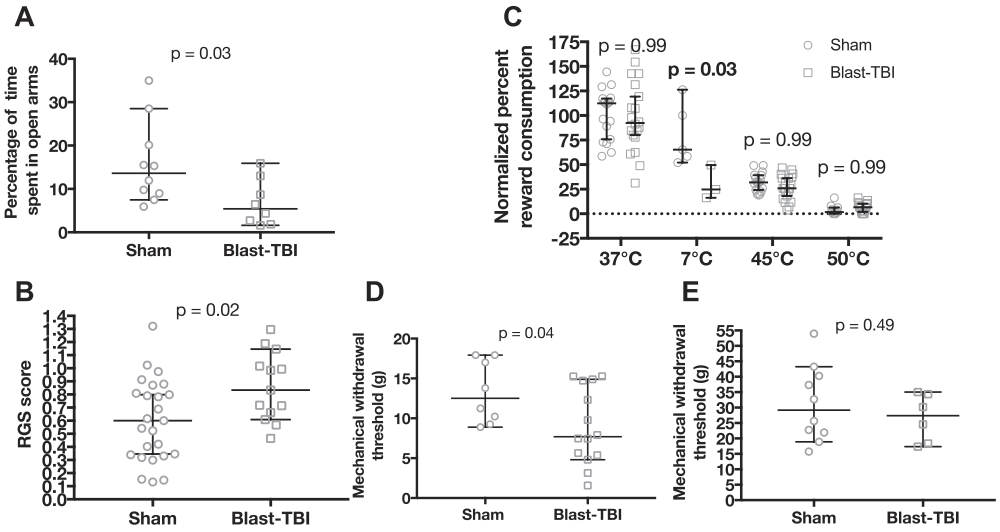

Fig. 3. Blast-TBI rats have persistent anxiety, ongoing pain, and cold hyperalgesia. All tests were performed 3–5 weeks after blast or sham treatments. A: **Anxiety**. Time spent in open arms of the elevated plus maze was significantly reduced in blast-TBI rats. B: **Ongoing pain**: Rat Grimace Scale scores in blast-TBI rats are significantly higher. C: **Cold hyperalgesia**: Rats with blast-TBI drank significantly less reward at 7 °C, normalized to individual reward consumption at the innocuous temperature of 37 °C, than sham rats, but consumed similar reward at the noxiously hot temperatures of 45 °C and 50 °C. D: **Tactile sensitivity**: Mechanical withdrawal thresholds to stimuli applied to the face were significantly lower in blast-injured rats. E: Compared to sham rats, blast-TBI rats did not have significantly different hind-paw withdrawal thresholds.

3.3.1. *Facial hyperalgesia*

We assessed sensitivity to noxious stimuli applied to the face by using an operant test of thermal sensitivity, the Orofacial Pain Assessment Device (OPAD) (Neubert et al., 2006). The OPAD establishes an operant conflict paradigm that creates a behavioral outcome where an animal must decide between receiving a reward and escaping a noxious stimulus. Unlike traditional reflexive tests, this operant test uses behavioral strategies that depend on cortical processing of input from pain pathways and does not rely on the experimenter's bias (Neubert et al., 2006).

We assessed facial thermal hyperalgesia with the OPAD. Because the maximum reward consumption varied by animal, for analysis of group data we normalized reward consumption to the proportion of reward consumed at the innocuous testing temperature of 37 °C. Fig. 3 compares normalized reward consumed by sham and blast-TBI rats at each of the testing temperatures. At 7 °C, rats in the sham group (n = 18) consumed approximately 62% of reward (median = 61.8, 95% CI = 0.5–126.2), whereas rats with blast-TBI (n = 20, median = 24.7%, 95% CI = 16.1–49.6) consumed only about 25% of their innocuous baseline consumption (two-way ANOVA, p = 0.03). There was no significant difference in consumption at 45 °C between blast-TBI (median = 25.9%, 95% CI = 18.0–36.3) and sham rats (median = 31.9%, 95% CI = 24.3–39.3; two-way ANOVA; p = 0.99). Similarly, at 50 °C, both groups had similar levels of low reward consumption (median = 1.75%, 95% CI = 0–6.25; blast-TBI median = 6.52, 95% CI = 1.96–10.32; two-way ANOVA, p = 0.99). These results suggest that blast-TBI in rats results in persistent facial hypersensitivity to cold temperatures.

In addition to thermal hypersensitivity, rats with TBI also displayed facial mechanical hyperalgesia (Fig. 3). Blast-TBI rats (n = 14) had a significantly lower withdrawal threshold to mechanical stimuli (median = 7.7 g; 95% CI = 4.8–14.9 g), compared to sham rats (n = 8; median = 12.5 g; 95% CI = 10.0–16.5; Mann-Whitney U = 26; p = 0.04).

3.3.2. *Hind-paw hyperalgesia*

To test whether rats with blast-TBI developed hyperalgesia to uninjured extremities of the body, we tested for responses to mechanical stimuli by applying von Frey filaments to the plantar surface of hind-paws. Fig. 3 compares hind-paw withdrawal thresholds of blast-TBI rats (n = 8) and sham rats (n = 14). There was no significant difference in withdrawal threshold between the groups (blast: median = 27.39 g; 95% CI = 17.33–35.02 vs. sham median = 29.18 g; 95% CI = 18.9–43.22; Mann-Whitney U = 23; p = 0.49). These results indicate that rats with blast-TBI do not exhibit distal mechanical hyperalgesia 3–4 weeks after blast-injury.

3.4. *Neuronal responses in the thalamus after blast-TBI*

Chronic pain after spinal cord injury is causally related to amplified neuronal activity in the posterior nucleus of the thalamus (PO; see Introduction). As previously reported (Masri and Keller, 2012; Poggio and Mountcastle, 1960), the receptive fields of PO neurons included not only the trigeminal innervaton area, but typically also included other somatic regions, often bilaterally. Although we did not quantify receptive field sizes, there was no apparent difference in the size of receptive fields in sham compared to blast-TBI rats.

To test if trigeminal hyperalgesia after blast-TBI involves similar mechanisms, we recorded spontaneous and evoked activity of PO neurons (see Methods). Typical of PO neurons in control animals (Masri et al., 2009; Trageser and Keller, 2004; Wu et al., 2013), the unit depicted in Fig. 4 (sham) exhibited relatively low spontaneous activity (1.52 Hz). In contrast, the unit recorded from the blast-TBI rat (Fig. 4) had a higher spontaneous firing rate (4.05 Hz). We recorded from 107 neurons in 11 blast-TBI rats and averaged data obtained from all cells recorded from an individual animal (see Methods). The median spontaneous firing rates in these animals was 1.8 Hz (95% CI = 1.2–2.9 Hz). In 11 sham rats we recorded from 79 neurons, and their median spontaneous firing rate was 1.5 Hz (95% CI = 0.9–2.7 Hz). These differences were not statistically significant (Mann-Whitney U = 38; p = 0.15; Fig. 4).

Similarly, there were no significant differences (Mann-Whitney U = 17; p = 0.9) between response magnitudes of neurons from sham (n = 6 rats, 37 neurons) and blast-TBI (n = 6 rats, 31 neurons) animals to noxious mechanical stimulation of the face (Fig. 4). Median response magnitude was 0.05 spikes/stimulus in blast-TBI rats (95% CI = 0.04–0.11) and 0.05 spikes/stimulus (95% CI = 0.02–0.22) in sham rats.

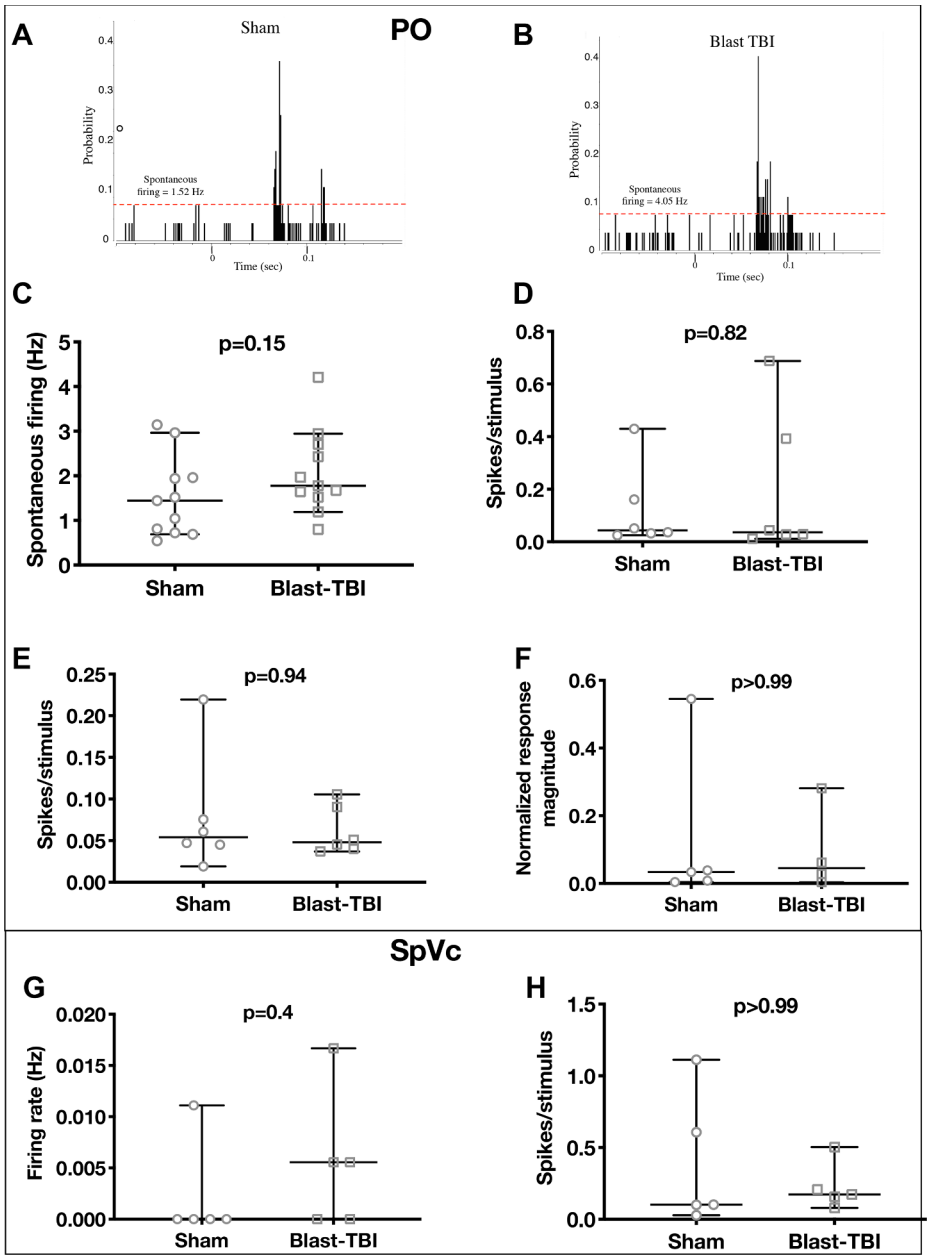

Fig. 4. Spontaneous and sensory-evoked neuronal activity in the posterior thalamus (PO) and in spinal trigeminal nucleus caudalis (SpVc) is unaffected in rats with blast-TBI. A, B: Representative PSTHs (1 ms bins) demonstrate spontaneous and noxious sensory-evoked activity of a PO neuron from a sham rat (A) and a blast- TBI rat (B). Horizontal lines depict 99% confidence intervals. C: Spontaneous firing rates were indistinguishable in blast-TBI rats compared to sham rats. D: Sensory-evoked responses to innocuous stimuli are not significantly different between blast- TBI and sham conditions. E, F: Sensory-evoked responses to noxious mechanical (E) and thermal (F) stimuli to the face are indistinguishable in neurons of blast-TBI and sham-injured rats. G, H: Median spontaneous firing rates (G) and sensory-evoked firing (H) are not significantly different in SpVc of blast-TBI rats, compared to sham rats.

We also compared the PO response to noxious heat applied to the face (see Methods). In blast-TBI rats (n = 4 rats, 6 neurons) the median normalized response magnitude was 0.05 (95% CI = 0.004–0.28), while cells in sham rats (n = 5 rats, 8 neurons) it was 0.03 units (95% CI = 0.004–0.55). The thermal responses, like the mechanical responses, were indistinguishable between the two conditions (Mann-Whitney U = 10; p > 0.99, Fig. 4). Thus, the response of PO cells to noxious mechanical and thermal stimulation was not altered by blast-TBI.

3.5. Neuronal responses in the trigeminal nucleus

We recorded activity in the spinal trigeminal nucleus caudalis (SpVc), which receives thermal and noxious inputs from the trigeminal nerve (Rusu, 2004) and is the main source of afferent inputs to the PO (Rowe and Sessle, 1968; Poggio and Mountcastle, 1960; Apkarian and Shi, 1994). We recorded spontaneous and stimulus-evoked responses from wide dynamic range (WDR) neurons that had receptive fields in the trigeminal dermatome (see Methods). In both sham and TBI rats, the receptive fields of these neurons were confined to the trigeminal innervation, and were constrained to one of the three dermatomes innervated by this nerve. We explored responses to superficial tactile and noxious stimuli, but did not attempt to obtain responses from deep cranial tissues. WDR neurons were identified by their responses to both low-threshold and noxious mechanical stimuli, and their enhanced responses to increases in stimulus intensity in the noxious range (Okubo et al., 2013). Consistent with previous findings (Okubo et al., 2013; Urch and Dickenson, 2003), spontaneous activity in sham rats was close to 0 Hz (n = 39 cells from 5 rats, median = 0.006, 95% CI = 0–0.02 Hz). Spontaneous activity was not significantly different in rats with blast-TBI (n = 34 cells from 5 rats, median = 0 Hz, 95% CI = 0–0.01 Hz; Mann-Whitney U = 8, p = 0.4; Fig. 4).

Similarly, the magnitude of responses to noxious mechanical stimuli applied to the face by an electronic esthesiometer was indistinguishable in both groups, with normalized response magnitudes of 0.17 spikes/stimulus in the blast-TBI group (n = 18 neurons from 5 rats, 95% CI = 0.08–0.50) and 0.10 spikes/stimulus in the sham group (n = 20 neurons from 5 rats, median = 0.10, 95% CI = 0.03–1.11; Mann-

Whitney U = 12, p > 0.99; Fig. 4). These results indicate that, 4 weeks after blast-TBI, WDR neurons in the SpVc of blast-TBI rats have activity comparable to that of sham controls.

3.6. Changes in glia after blast-TBI

While ascending sensory pain information travels through the PO, downstream processing and descending modulation are transmitted through the PAG and RVM, which also show aberrant activity in chronic pain states. Higher activity in PO may correlate with inflammation in these downstream descending pain modulatory centers. PAG may be particularly susceptible to our new blast-TBI model, because we aimed the collimated blast wave over the occipital crest, which likely induced a hydrostatic pulse within the CSF at the foramen magnum that traveled through the fourth ventricle and aqueduct of Sylvius, affecting the surrounding PAG. We and others have shown that some CNS injuries are associated with activation of glia in thalamus (Wu et al., 2013; Hazra et al., 2014; Ramlackhansingh et al., 2011). However, densitometry analysis revealed no significant differences in intensity of GFAP immunoreactivity in PO of blast-TBI rats, compared to shams, at either 2 days (blast-TBI: n = 5, median = 0.65, 95% CI = 0.10–1.10; sham: n = 3, median = 1.01, 95% CI = 0.41–1.58; U = 4, p = 0.39) or 60 days post-injury (blast-TBI: n = 4, median = 1.29, 95% CI = 0.32–1.40; sham: n = 4, median = 1.00, 95%CI = 0.45–1.54; U = 7, p = 0.89; Fig. 5). Nor did we find changes in Iba1 stereological cell counts within PO at the 2 day (blast-TBI: n = 5, median = 0.81, 95% CI = 0.30–1.15; sham: n = 3, median = 0.98, 95% CI = 0.18–1.84; U = 7, p = 0.99) or 60 day time points (blast-TBI: n = 3, median = 0.99, 95%CI = 0.58–2.32; sham: n = 3, median = 1.13, 95%CI = 0.62–1.25; U = 4, p = 0.99; Fig. 5).

Gliosis upstream of the thalamus, in SpVc, could also mediate thalamic abnormalities. However, there were no significant changes in percent of the ROI field labeled positively for GFAP in the SpVc of blast-TBI rats at 2 days (blast-TBI: n = 5, median = 1.17, 95% CI = 0.99–1.78; sham: n = 4, median = 0.99, 95% CI = 0.80–1.23; U = 4, p = 0.19) or 60 days (blast-TBI: n = 6, median = 1.73, 95% CI = 0.82–2.47; sham: n = 4, median = 1.19, 95% CI = 0.37–1.26; U = 3, p = 0.07; Fig. 5) after blast-TBI. The number of Iba1-labeled cells was also indistinguishable 60 days after injury (blast-TBI: n = 5, median = 0.31, 95% CI = 0.18–2.45; sham: n = 3, median = 0.65, 95% CI = 0.23–2.12; U = 7, p = 0.99; Fig. 5).

3.6.1. Gliosis in descending modulatory centers after blast-TBI

Due to its importance for pain modulation and susceptibility to blast trauma (see Introduction), we examined gliosis in the periaqueductal gray (PAG) and its downstream target in the brainstem, the rostroventral medulla (RVM). Sections containing the PAG and RVM were labeled for GFAP and Iba1 at 16 weeks after injury to quantify and classify astrocytes and microglia, respectively. Sham (n = 4) and blast-TBI rats (n = 6) had similar integrated densities of GFAP labeling in both the PAG (sham: median = 1074, 95% CI = 766–1228; blast-TBI: median = 1207, 95% CI = 1044–1380; U = 6, p = 0.26; Fig. 6) and RVM (sham: median = 925, 95% CI = 627–1277; blast-TBI: median = 982, 95% CI = 925–1224; U = 9, p = 0.61; Fig. 6). Thus, persistent gliosis in the descending pain modulatory centers does not mediate ongoing pain at late time-points after blast-TBI.

4. Discussion

4.1. Blast-TBI in awake rats as a model for human injury

We developed a novel model of blast-TBI, adapted from our previously described direct cranial blast injury (dcBI) model (Kuehn et al., 2011). The model resembles human injury by removing the use of anesthetics or surgery that are common in other rodent models of TBI. Craniotomies alone—without brain damage—can produce profound pro-inflammatory, morphological, and behavioral deficits that may confound interpretation of results in conventional experimental brain injury models (Cole et al., 2011; Kurland et al., 2015). Anesthesia may produce neuroprotective effects that mask the nerve damage initiated by blast-TBI, a crucial step for the development of central pain (Freynhagen and Baron, 2009). Anesthetics may also reduce neuronal activity and brain inflammation (Combes, 2013; Hertle et al., 2012). Even a brief, 15-minute exposure to isoflurane is sufficient to reduce secondary injury and inflammation after controlled cortical impact (Luh et al., 2011). Thus, variability in long-term outcomes in preclinical TBI studies is influenced by the anesthetic used at time of injury.

The present findings differ somewhat from those we recently reported using the same bTBI approach in ketamine-xylazine anesthetized rats (Studlack et al., 2018). While the system used to produce the blast injury is identical in both studies, mortality is lower (3.7% vs. 1.3%) when animals are awake, possibly due to detrimental effects of the anesthetics, such as respiratory depression. In addition, rats exposed to blast-TBI under anesthesia developed persistent mechanical hyperalgesia of the face (Studlack et al., 2018), a finding not replicated in the present, awake blast-TBI study. This may be due to tighter coupling between the blast dissipation chamber and the rat's head when anesthetized, resulting in more efficient blast wave dissipation in the anesthetized model. Unlike the awake rats reported here, anesthetized rats did not display increased anxiety-like behavior—measured in an elevated plus maze (Studlack et al., 2018)—suggesting that anesthesia may mask the development of co-morbid anxiety in some models of blast-TBI.

Warfighters equipped with helmet and body armor typically have the suboccipital/upper cervical region completely unprotected from a blast wave originating from behind them – the very scenario we modeled in the aforementioned paper and used here in awake rats. By contrast, shock-tube blast exposes the entire body (if completely unprotected), which is not the typical scenario for war fighters with armor. The awake blast-TBI model presented here recapitulates multiple behavioral aspects of the human condition at the time of primary blast injury, making it a more relevant rodent model for future study than models using anesthetics at time of injury.

4.2. Pain and thalamic activity after blast-TBI

Blast-TBI in humans is associated with increased sensitivity to painful stimuli and chronic pain, particularly in the head and back (Rosenfeld et al., 2013; Sayer, 2012; Tham et al., 2013). To determine if similar outcomes occur in our animal model, we compared blast-TBI and sham rats with tests of ongoing pain and hyperalgesia. Rats with blast-TBI displayed signs of persistent pain, i.e., elevated grimace scores (Fig. 3B) and increased sensitivity to hypothermia, assessed using an operant conditioning task (Fig. 3C). Our findings are consistent with data on patients with TBI, showing that they suffer not only from post-traumatic headaches, but also generalized pain, including aberrant hypersensitivity to cold (Ofek and Defrin, 2007; Nampiaparampil, 2008; Strigo et al., 2014).

We disproved our hypothesis that chronic pain after blast-TBI results from amplified activity of neurons in the PO thalamus. Neither the spontaneous nor the evoked responses of PO neurons were significantly affected by blast-TBI. These findings are in contrast with our previous reports of increased spontaneous firing of thalamic neurons and aberrant thalamocortical connectivity in animals with pain after SCI (Masri et al., 2009; Seminowicz et al., 2012; Whitt et al., 2013; Wu et al., 2013). We also found no significant changes in the activity of SpVc neurons, which receive direct inputs from trigeminal afferents. It is possible that the subset of all SpVc neurons recorded in our study do not reflect changes produced by the blast-TBI; however, we did not directly address this possibility. Thus, the persistent neurophysiological changes causing the chronic pain in our blast-TBI model remain unknown.

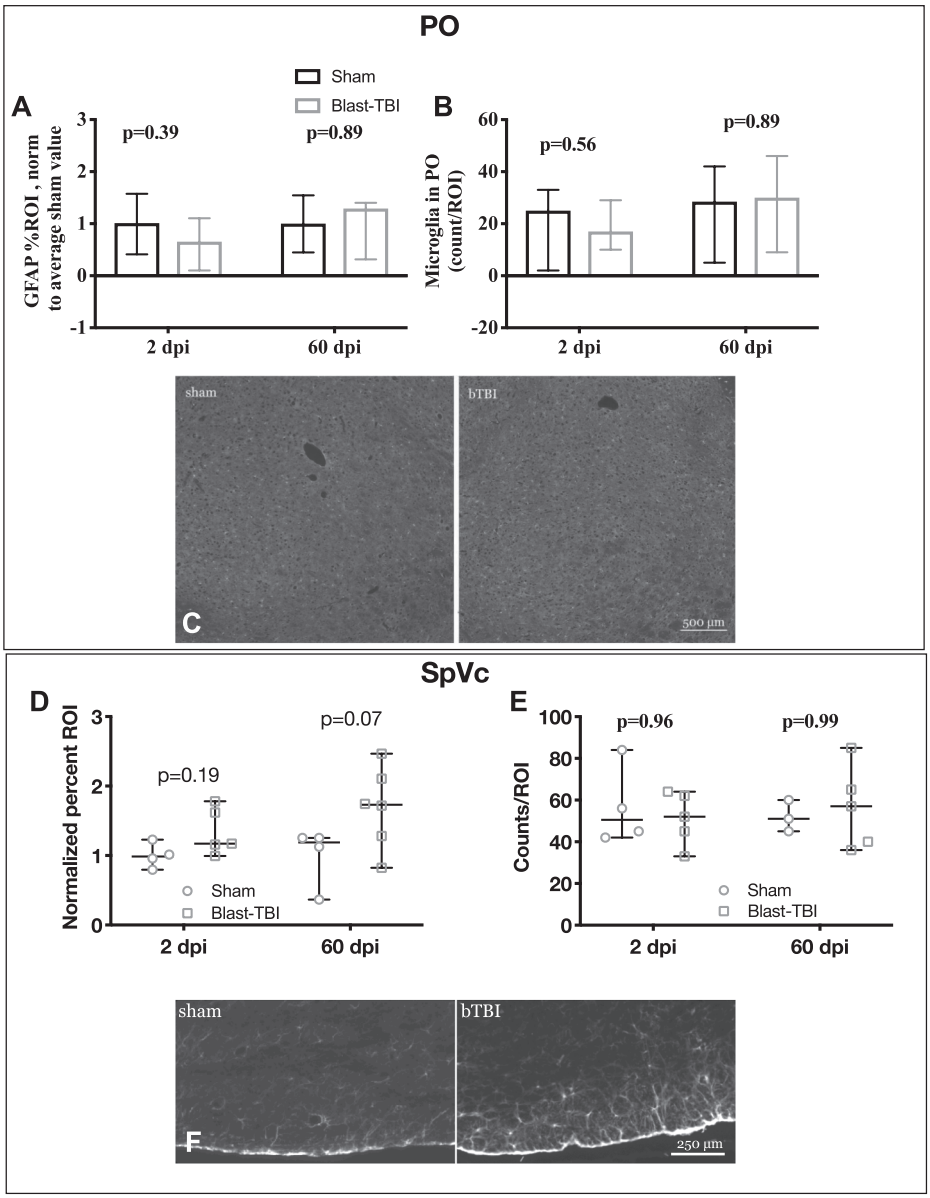

Fig. 5. Glial markers in the posterior thalamus (PO) and in spinal trigeminal nucleus caudalis (SpVc) are unaffected in rats with blast-TBI. A: GFAP labeling in PO shows no significant difference in percent ROI between sham and blast-TBI rats, at either short-term or long-term time-points post-injury. B: Number of Iba1-positive cells in sham and blast-TBI rats was not different at 2 days post-injury (dpi) or 60 dpi. C: Representative micrographs of histological samples. D: Similarly, in SpVc, GFAP labeling shows no significant difference in percent ROI between sham and blast-TBI rats at either 2 dpi or 60 dpi. E: Cell counts of Iba1 labeled microglia in the brainstem show no significant difference in population size at 2 dpi or 60 dpi. F: Representative micrographs of histological samples.

4.3. Inflammatory gliosis in thalamus after TBI

We hypothesized that the aberrant elevated PO activity after injury reported by others was caused by inflammatory factors from activated glia, sensitizing PO neurons (Scholz and Woolf, 2007; Milligan and Watkins, 2009; Ren and Dubner, 2008). Contrary to our hypothesis, we found no changes in resting-state glial cells at either time-point. These findings are consistent with reports that glial activation is limited to areas of neurodegeneration (Readnower et al., 2010; Gama Sosa et al., 2014; Garman et al., 2011).

However, these findings are in contrast with previous TBI studies that detected inflammatory damage in the thalamus. In rodents with fluid percussion injury (Cao et al., 2012) model of TBI, Cao et al (2012) reported that sensory deficits are associated with thalamic microglial activation lasting 1 week after injury. Hazra et al. (2014) demonstrated thalamic astrogliosis in mice up to 4 weeks after controlled cortical impact. However, mice with thalamic astrogliosis did not exhibit altered pain behaviors (Hazra et al., 2014; Vos et al., 1994). These results might differ from our findings due to the use of different TBI models. They might also be confounded by the use of anesthesia, craniotomy and direct brain impact in these invasive, non-blast TBI models.

The absence of activated glia in the thalamus was not unexpected, due to the orientation of the blast wave and the nature of primary blast injury to brain tissue. We directed the blast wave over the brainstem, caudal to the thalamus, which was not in the direct path of the collimated wave. Additionally, tissue at the borders of a material with different density are particularly susceptible to blast injury, noted by glial scarring (Shively et al., 2016; Nakagawa et al., 2011). The thalamus, situated towards the center of the brain mass, may be largely protected from local effects of primary blast injury. However, although we observed persistent behavioral markers of pain and hyperalgesia, there was no aberrant PO activity, leading us to examine other potential sources of maladaptive responses after blast-TBI.

We assessed persistent glial-mediated inflammation (Watkins et al., 2001) in the PAG or RVM, key structures in the descending pain modulatory pathway (Basbaum and Fields, 1978; Reynolds, 1969; Tsou and Jang, 1964). We found no disparities in glial labeling 16 weeks after injury, suggesting that if chronic pain is mediated by gliosis in PAG and RVM, it is a transient process that abates by the time we tested. We conclude that persistent ongoing pain is maintained through other mechanisms that remain to be identified.

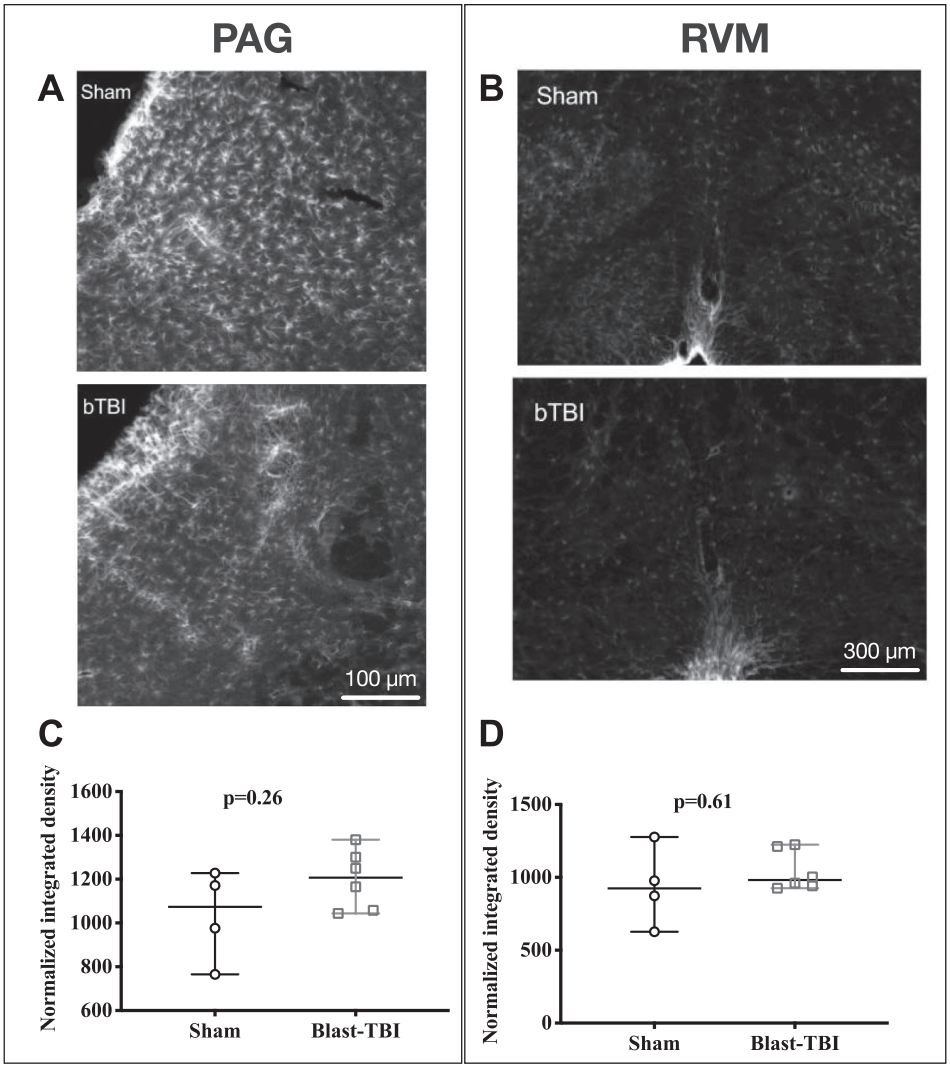

Fig. 6. Astrogliosis is not increased in the PAG or RVM 16 weeks after blast-TBI. A, B: Representative images of GFAP in PAG (A) and RVM (B) show comparable labeling in sham (top) and blast-injured rats (bottom). C: Sham and blast-TBI rats have similar amounts of GFAP labeling in PAG. D: GFAP labeling was also similar between groups in RVM.

5. Conclusions

We developed an awake-rat explosive blast-induced traumatic brain injury (blast-TBI) that eliminates complications associated with anesthesia and surgery in other TBI models. Rats with blast-TBI developed ongoing, spontaneous pain. This novel model will enable future studies on the pathophysiology of chronic pain after blast-TBI, and other sequelae of this devastating condition.

Author contributions

OU,PES,SP,KK,AC,TF,NS collected data; NS,PES,SP,AK analyzed data; PES,SP,VG,JMS,AK designed experiments.

Funding

This work was supported by the U.S. Department of Veterans Affairs [5I01BX001629; I01BX002889] and National Institutes of Health [5R01NS099245; R01NS102589)]. The supporting agencies had no involvement in study design, data interpretation, writing, or submission of this manuscript.

Conflict of interest

The authors report no conflict of interest.

Appendix A. Supplementary data

Supplementary data to this article can be found online at https://doi.org/10.1016/j.ynpai.2019.100030.

References

Akintola, T., Raver, C., Studlack, P., Uddin, O., Masri, R., Keller, A., 2017. The grimace scale reliably assesses chronic pain in a rodent model of trigeminal neuropathic pain. Neurobiol. Pain 213–217.

Apkarian, A.V., Shi, T., 1994. Squirrel monkey lateral thalamus. I. Somatic nociresponsive neurons and their relation to spinothalamic terminals. J. Neurosci. 14 (11 Pt 2), 6779–6795.

Bannister, K., Dickenson, A.H., 2017. The plasticity of descending controls in pain: translational probing. J. Physiol. 595 (13), 4159–4166.

Basbaum, A.I., Fields, H.L., 1978. Endogenous pain control mechanisms: review and hypothesis. Ann. Neurol. 4 (5), 451–462.

Belanger, H.G., Uomoto, J.M., Vanderploeg, R.D., 2009. The Veterans Health Administration's (VHA's) polytrauma system of care for mild traumatic brain injury: costs, benefits, and controversies. J. Head Trauma Rehabil. 24 (1), 4–13.

Burstein, R., Jakubowski, M., Garcia-Nicas, E., Kainz, V., Bajwa, Z., Hargreaves, R., Becerra, L., Borsook, D., 2010. Thalamic sensitization transforms localized pain into

widespread allodynia. Ann. Neurol. 68 (1), 81–91.
Cao, T., Thomas, T.C., Ziebell, J.M., Pauly, J.R., Lifshitz, J., 2012. Morphological and genetic activation of microglia after diffuse traumatic brain injury in the rat. Neuroscience 22565–22575.
Cernak, I., Noble-Haeusslein, L.J., 2010. Traumatic brain injury: an overview of pathobiology with emphasis on military populations. J. Cereb. Blood Flow Metab. 30 (2), 255–266.
Cole, J.T., Yarnell, A., Kean, W.S., Gold, E., Lewis, B., Ren, M., McMullen, D.C., Jacobowitz, D.M., Pollard, H.B., O'Neill, J.T., Grunberg, N.E., Dalgard, C.L., Frank, J.A., Watson, W.D., 2011. Craniotomy: true sham for traumatic brain injury, or a sham of a sham. J. Neurotrauma 28 (3), 359–369.
Combes, R.D., 2013. A critical review of anaesthetised animal models and alternatives for military research, testing and training, with a focus on blast damage, haemorrhage and resuscitation. Altern. Lab. Anim. 41 (5), 385–415.
De Rantere, D., Schuster, C.J., Reimer, J.N., Pang, D.S., 2016. The relationship between the Rat Grimace Scale and mechanical hypersensitivity testing in three experimental pain models. Eur. J. Pain 20 (3), 417–426.
Dixon, W.J., 1965. The up-and-down method for small samples. J. Am. Stat. Assoc. 60 (312), 967–978.
Dobscha, S.K., Clark, M.E., Morasco, B.J., Freeman, M., Campbell, R., Helfand, M., 2009. Systematic review of the literature on pain in patients with polytrauma including traumatic brain injury. Pain Med. 10 (7), 1200–1217.
Elder, G.A., Mitsis, E.M., Ahlers, S.T., Cristian, A., 2010. Blast-induced mild traumatic brain injury. Psychiatr. Clin. North Am. 33 (4), 757–781.
Freynhagen, R., Baron, R., 2009. The evaluation of neuropathic components in low back pain. Curr. Pain Headache Rep. 13 (3), 185–190.
Friedberg, M.H., Lee, S.M., Ebner, F.F., 1999. Modulation of receptive field properties of thalamic somatosensory neurons by the depth of anesthesia. J. Neurophysiol. 81 (5), 2243–2252.
Gama Sosa, M.A., De Gasperi, R., Janssen, P.L., Yuk, F.J., Anazodo, P.C., Pricop, P.E., Paulino, A.J., Wicinski, B., Shaughness, M.C., Maudlin-Jeronimo, E., Hall, A.A., Dickstein, D.L., McCarron, R.M., Chavko, M., Hof, P.R., Ahlers, S.T., Elder, G.A., 2014. Selective vulnerability of the cerebral vasculature to blast injury in a rat model of mild traumatic brain injury. Acta Neuropathol. Commun. 267.
Garman, R.H., Jenkins, L.W., Switzer, R.C., Bauman, R.A., Tong, L.C., Swauger, P.V., Parks, S.A., Ritzel, D.V., Dixon, C.E., Clark, R.S., Bayir, H., Kagan, V., Jackson, E.K., Kochanek, P.M., 2011. Blast exposure in rats with body shielding is characterized primarily by diffuse axonal injury. J. Neurotrauma 28 (6), 947–959.
Hara, K., Harris, R.A., 2002. The anesthetic mechanism of urethane: the effects on neurotransmitter-gated ion channels. Anesth. Analg. 94 (2), 313–318 table of contents.
Hayman, E., Keledjian, K., Stokum, J.A., Pampori, A., Gerzanich, V., Simard, J.M., 2018. Selective vulnerability of the foramen magnum in a rat blast traumatic brain injury model. J. Neurotrauma 35 (17), 2136–2142.
Hazra, A., Macolino, C., Elliott, M.B., Chin, J., 2014. Delayed thalamic astrocytosis and disrupted sleep-wake patterns in a preclinical model of traumatic brain injury. J. Neurosci. Res. 92 (11), 1434–1445.
Heinricher, M.M., Tavares, I., Leith, J.L., Lumb, B.M., 2009. Descending control of nociception: Specificity, recruitment and plasticity. Brain Res. Rev. 60 (1), 214–225.
Hertle, D.N., Dreier, J.P., Woitzik, J., Hartings, J.A., Bullock, R., Okonkwo, D.O., Shutter, L.A., Vidgeon, S., Strong, A.J., Kowoll, C., Dohmen, C., Diedler, J., Veltkamp, R., Bruckner, T., Unterberg, A.W., Sakowitz, O.W., Cooperative Study of Brain Injury Depolarizations, C.O.S.B.I.D., 2012. Effect of analgesics and sedatives on the occurrence of spreading depolarizations accompanying acute brain injury. Brain 135 (Pt 8), 2390–2398.
Jang, S.H., Park, S.M., Kwon, H.G., 2016. Relation between injury of the periaqueductal gray and central pain in patients with mild traumatic brain injury: observational study. Medicine (Baltimore) 95 (26), e4017.
Kapinya, K.J., Prass, K., Dirnagl, U., 2002. Isoflurane induced prolonged protection against cerebral ischemia in mice: a redox sensitive mechanism. NeuroReport 13 (11), 1431–1435.
Keller, A., Masri, R., 2014. Thalamocortical abnormalities in spinal cord injury pain. In: Saab, C.Y. (Ed.), Chronic Pain and Brain Abnormalities. Elsevier, Amsterdam, pp. 95–125.
Kuehn, R., Simard, P.F., Driscoll, I., Keledjian, K., Ivanova, S., Tosun, C., Williams, A., Bochicchio, G., Gerzanich, V., Simard, J.M., 2011. Rodent model of direct cranial blast injury. J. Neurotrauma 28 (10), 2155–2169.
Kurland, D.B., Khaladj-Ghom, A., Stokum, J.A., Carusillo, B., Karimy, J.K., Gerzanich, V., Sahuquillo, J., Simard, J.M., 2015. Complications associated with decompressive craniectomy: a systematic review. Neurocrit. Care 23 (2), 292–304.
Langford, D.J., Bailey, A.L., Chanda, M.L., Clarke, S.E., Drummond, T.E., Echols, S., Glick, S., Ingrao, J., Klassen-Ross, T., Lacroix-Fralish, M.L., Matsumiya, L., Sorge, R.E., Sotocinal, S.G., Tabaka, J.M., Wong, D., van den Maagdenberg, A.M., Ferrari, M.D., Craig, K.D., Mogil, J.S., 2010. Coding of facial expressions of pain in the laboratory mouse. Nat. Methods 7 (6), 447–449.
Lee, H., Wintermark, M., Gean, A.D., Ghajar, J., Manley, G.T., Mukherjee, P., 2008. Focal lesions in acute mild traumatic brain injury and neurocognitive outcome: CT versus 3T MRI. J. Neurotrauma 25 (9), 1049–1056.
Lew, H.L., Otis, J.D., Tun, C., Kerns, R.D., Clark, M.E., Cifu, D.X., 2009. Prevalence of chronic pain, posttraumatic stress disorder, and persistent postconcussive symptoms in OIF/OEF veterans: polytrauma clinical triad. J. Rehabil. Res. Dev. 46 (6), 697–702.
Luh, C., Gierth, K., Timaru-Kast, R., Engelhard, K., Werner, C., Thal, S.C., 2011. Influence of a brief episode of anesthesia during the induction of experimental brain trauma on secondary brain damage and inflammation. PLoS One 6 (5), e19948.
Mason, P., 2011. From descending pain modulation to obesity via the medullary raphe. Pain 152 (3 Suppl.), S20–S24.
Masri, R., Bezdudnaya, T., Trageser, J.C., Keller, A., 2008. Encoding of stimulus frequency and sensor motion in the posterior medial thalamic nucleus. J. Neurophysiol. 100 (2), 681–689.
Masri, R., Quiton, R.L., Lucas, J.M., Murray, P.D., Thompson, S.M., Keller, A., 2009. Zona incerta: a role in central pain. J. Neurophysiol. 102 (1), 181–191.
Masri, R., Keller, A., 2012. Chronic pain following spinal cord injury. Adv. Exp. Med. Biol. 76074–76088.
Matsumiya, L.C., Sorge, R.E., Sotocinal, S.G., Tabaka, J.M., Wieskopf, J.S., Zaloum, A., King, O.D., Mogil, J.S., 2012. Using the Mouse Grimace Scale to reevaluate the efficacy of postoperative analgesics in laboratory mice. J. Am. Assoc. Lab. Anim. Sci. 51 (1), 42–49.
Milligan, E.D., Watkins, L.R., 2009. Pathological and protective roles of glia in chronic pain. Nat. Rev. Neurosci. 10 (1), 23–36.
Mogil, J.S., 2009. Animal models of pain: progress and challenges. Nat. Rev. Neurosci. 10 (4), 283–294.
Nakagawa, A., Manley, G.T., Gean, A.D., Ohtani, K., Armonda, R., Tsukamoto, A., Yamamoto, H., Takayama, K., Tominaga, T., 2011. Mechanisms of primary blast-induced traumatic brain injury: insights from shock-wave research. J. Neurotrauma 28 (6), 1101–1119.
Nampiaparampil, D.E., 2008. Prevalence of chronic pain after traumatic brain injury: a systematic review. JAMA 300 (6), 711–719.
Neubert, J.K., Rossi, H.L., Malphurs, W., Vierck, C.J., Caudle, R.M., 2006. Differentiation between capsaicin-induced allodynia and hyperalgesia using a thermal operant assay. Behav. Brain Res. 170 (2), 308–315.
Noseda, R., Burstein, R., 2013. Migraine pathophysiology: anatomy of the trigeminovascular pathway and associated neurological symptoms, CSD, sensitization and modulation of pain. Pain 154 (Suppl.), 1.
Ofek, H., Defrin, R., 2007. The characteristics of chronic central pain after traumatic brain injury. Pain 131 (3), 330–340.
Okubo, M., Castro, A., Guo, W., Zou, S., Ren, K., Wei, F., Keller, A., Dubner, R., 2013. Transition to persistent orofacial pain after nerve injury involves supraspinal serotonin mechanisms. J. Neurosci. 33 (12), 5152–5161.
Ossipov, M.H., Morimura, K., Porreca, F., 2014. Descending pain modulation and chronification of pain. Curr. Opin. Support Palliat. Care 8 (2), 143–151.
Park, E., Bell, J.D., Siddiq, I.P., Baker, A.J., 2009. An analysis of regional microvascular loss and recovery following two grades of fluid percussion trauma: a role for hypoxia-inducible factors in traumatic brain injury. J. Cereb. Blood Flow Metab. 29 (3), 575–584.
Patil, V.K., St Andre, J.R., Crisan, E., Smith, B.M., Evans, C.T., Steiner, M.L., Pape, T.L., 2011. Prevalence and treatment of headaches in veterans with mild traumatic brain injury. Headache 51 (7), 1112–1121.
Poggio, G.F., Mountcastle, V.B., 1960. A study of the functional contributions of the lemniscal and spinothalamic systems to somatic sensibility. Central nervous mechanisms in pain. Bull. Johns Hopkins Hosp. 106, 266–316.
Polusny, M.A., Kehle, S.M., Nelson, N.W., Erbes, C.R., Arbisi, P.A., Thuras, P., 2011. Longitudinal effects of mild traumatic brain injury and posttraumatic stress disorder comorbidity on postdeployment outcomes in national guard soldiers deployed to Iraq. Arch. Gen. Psychiatry 68 (1), 79–89.
Ramlackhansingh, A.F., Brooks, D.J., Greenwood, R.J., Bose, S.K., Turkheimer, F.E., Kinnunen, K.M., Gentleman, S., Heckemann, R.A., Gunanayagam, K., Gelosa, G., Sharp, D.J., 2011. Inflammation after trauma: microglial activation and traumatic brain injury. Ann. Neurol. 70 (3), 374–383.
Readnower, R.D., Chavko, M., Adeeb, S., Conroy, M.D., Pauly, J.R., McCarron, R.M., Sullivan, P.G., 2010. Increase in blood-brain barrier permeability, oxidative stress, and activated microglia in a rat model of blast-induced traumatic brain injury. J. Neurosci. Res. 88 (16), 3530–3539.
Ren, K., Dubner, R., 2008. Neuron-glia crosstalk gets serious: role in pain hypersensitivity. Curr. Opin. Anaesthesiol. 21 (5), 570–579.
Reynolds, D.V., 1969. Surgery in the rat during electrical analgesia induced by focal brain stimulation. Science 164 (3878), 444–445.
Rosenfeld, J.V., McFarlane, A.C., Bragge, P., Armonda, R.A., Grimes, J.B., Ling, G.S., 2013. Blast-related traumatic brain injury. Lancet Neurol. 12 (9), 882–893.
Rowe, M.J., Sessle, B.J., 1968. Somatic afferent input to posterior thalamic neurones and their axon projection to the cerebral cortex in the cat. J. Physiol. 196 (1), 19–35.
Ruff, R.L., Ruff, S.S., Wang, X.F., 2008. Headaches among Operation Iraqi Freedom/Operation Enduring Freedom veterans with mild traumatic brain injury associated with exposures to explosions. J. Rehabil. Res. Dev. 45 (7), 941–952.
Rusu, M.C., 2004. The spinal trigeminal nucleus–considerations on the structure of the nucleus caudalis. Folia Morphol. (Warsz) 63 (3), 325–328.
Sayer, N.A., 2012. Traumatic brain injury and its neuropsychiatric sequelae in war veterans. Annu. Rev. Med. 63405–63419.
Sceniak, M.P., Maciver, M.B., 2006. Cellular actions of urethane on rat visual cortical neurons in vitro. J. Neurophysiol. 95 (6), 3865–3874.
Scholz, J., Woolf, C.J., 2007. The neuropathic pain triad: neurons, immune cells and glia. Nat. Neurosci. 10 (11), 1361–1368.
Seminowicz, D.A., Jiang, L., Ji, Y., Xu, S., Gullapalli, R.P., Masri, R., 2012. Thalamocortical asynchrony in conditions of spinal cord injury pain in rats. J. Neurosci. 32 (45), 15843–15848.
Shively, S.B., Horkayne-Szakaly, I., Jones, R.V., Kelly, J.P., Armstrong, R.C., Perl, D.P., 2016. Characterisation of interface astroglial scarring in the human brain after blast exposure: a post-mortem case series. Lancet Neurol. 15 (9), 944–953.
Sotocinal, S.G., Sorge, R.E., Zaloum, A., Tuttle, A.H., Martin, L.J., Wieskopf, J.S., Mapplebeck, J.C., Wei, P., Zhan, S., Zhang, S., McDougall, J.J., King, O.D., Mogil, J.S., 2011. The Rat Grimace Scale: a partially automated method for quantifying pain in the laboratory rat via facial expressions. Mol. Pain 755.
Strigo, I.A., Spadoni, A.D., Lohr, J., Simmons, A.N., 2014. Too hard to control: compromised pain anticipation and modulation in mild traumatic brain injury. Transl.

Psychiatry 4e340.
Studlack, P.E., Keledjian, K., Farooq, T., Akintola, T., Gerzanich, V., Simard, J.M., Keller, A., 2018. Blast-induced brain injury in rats leads to transient vestibulomotor deficits and persistent orofacial pain. Brain Inj. 1–13.
Tang, H.L., Sun, H.P., Wu, X., Sha, H.Y., Feng, X.Y., Zhu, J.H., 2011. Detection of neural stem cells function in rats with traumatic brain injury by manganese- enhanced magnetic resonance imaging. Chin. Med. J. (Engl) 124 (12), 1848–1853.
Taylor, B.C., Hagel, E.M., Carlson, K.F., Cifu, D.X., Cutting, A., Bidelspach, D.E., Sayer, N.A., 2012. Prevalence and costs of co-occurring traumatic brain injury with and without psychiatric disturbance and pain among Afghanistan and Iraq War Veteran V.A. users. Med. Care 50 (4), 342–346.
Tham, S.W., Palermo, T.M., Wang, J., Jaffe, K.M., Temkin, N., Durbin, D., Rivara, F.P., 2013. Persistent pain in adolescents following traumatic brain injury. J. Pain 14 (10), 1242–1249.
Trageser, J.C., Keller, A., 2004. Reducing the uncertainty: gating of peripheral inputs by zona incerta. J. Neurosci. 24 (40), 8911–8915.
Tsou, K., Jang, C.S., 1964. Studies on the site of analgesic action of morphine by intracerebral micro-injection. Sci. Sin. 131099–131109.
Urch, C.E., Dickenson, A.H., 2003. In vivo single unit extracellular recordings from spinal cord neurones of rats. Brain Res. Brain Res. Protoc. 12 (1), 26–34.
Venkatesan, U.M., Dennis, N.A., Hillary, F.G., 2015. Chronology and chronicity of altered resting-state functional connectivity after traumatic brain injury. J. Neurotrauma 32 (4), 252–264.
Vos, B.P., Strassman, A.M., Maciewicz, R.J., 1994. Behavioral evidence of trigeminal neuropathic pain following chronic constriction injury to the rat's infraorbital nerve. J. Neurosci. 14 (5 Pt 1), 2708–2723.
Warner, D.S., Zhou, J.G., Ramani, R., Todd, M.M., 1991. Reversible focal ischemia in the rat: effects of halothane, isoflurane, and methohexital anesthesia. J. Cereb. Blood Flow Metab. 11 (5), 794–802.
Watkins, L.R., Milligan, E.D., Maier, S.F., 2001. Glial activation: a driving force for pathological pain. Trends Neurosci. 24 (8), 450–455.
Whitt, J.L., Masri, R., Pulimood, N.S., Keller, A., 2013. Pathological activity in mediodorsal thalamus of rats with spinal cord injury pain. J. Neurosci. 33 (9), 3915–3926.
Wu, J., Raver, C., Piao, C., Keller, A., Faden, A.I., 2013. Cell cycle activation contributes to increased neuronal activity in the posterior thalamic nucleus and associated chronic hyperesthesia after rat spinal cord contusion. Neurotherapeutics 10 (3), 520–538.
Zhu, Y., Li, Z., Bai, L., Tao, Y., Sun, C., Li, M., Zheng, L., Zhu, B., Yao, J., Zhou, H., Zhang, M., 2014. Loss of microstructural integrity in the limbic-subcortical networks for acute symptomatic traumatic brain injury. Biomed. Res. Int 2014548392.